Fusion of MR and SPECT Images Using Statistics based Guided Image Filter with Weighted Average Rule

Fathima Zaheera[1], Dr. SudhagarGovinda Swamy[2]

[1]Associate Professor,[2]Professor, Department of ECE

[1,2]Siddhartha Institute of Technology and Sciences, Narapally, Hyderabad, Telangana

ABSTRACT

A fast and effective image fusion method is proposed for creating a highly informative fused image through merging multiple images. The proposed method is based on a two-scale decomposition of an image into a base layer containing large scale variations in intensity, and a detail layer capturing small scale details. A novel Statistics based guided image filtering-based weighted average technique is proposed to make full use of spatial consistency for fusion of the base and detail layers. Experimental results demonstrate that the proposed method can obtain state-of-the-art performance for fusion of multispectral, multi focus, multimodal, and multi exposure images.

Keywords: MR imaging, SPECT imaging, medical image fusion, guided image filter, image statistics, weighted average fusion

1. INTRODUCTION

Image fusion treats the different combinations of images sensed from different sensors which include multi-spectrum and high-spectrum, multi-angle viewing and multi-resolutions. This enhances the scope for accomplishing the quality of images. Multi-sensor images are used in several fields such as machine vision, remote sensing and medical imaging. Medical image fusion techniques provide better biomedical information for clinical evaluation. In medical diagnosis multimodal fused images has more significant role than individual image. The multi model medical image fusion is the process of combining compliment fusion techniques for clinical analysis.

To support more accurate clinical information for physicians to deal with medical diagnosis and assessment, multimodality medical images are required such as Computed Tomography (CT), Magnetic Resonance Imaging (MRI), or Positron Emission Tomography (PET) [1,2] etc. For example, the CT image can provide dense structures like bones and implants with less distortion but cannot detect physiological changes. But the MRI can provide information of normal and pathological soft tissues and it cannot support the bone information. In this circumstance, a single image cannot be appropriate to deliver perfect clinical requirements for the physicians. Hence the fusion of the multimodal medical images is essential, and it has become a promising and very challenging research area in recent years [3].Image fusion broadly defined as the representation of the visual information with more than one input image, as a single fused image without the introduction of distortion or loss of information [4]. The fusion of different images can reduce the ambiguity related to a single image. In recent days, obtaining human's anatomies and functions with high resolution and more instructive description becomes potential due to

advancement in the field of medical imaging technology. The encouragement for the research in the analysis of medical images has been done by such development. In addition, the development of medical images vitality in the clinical applications rendered a straight effect on this field of research [5].

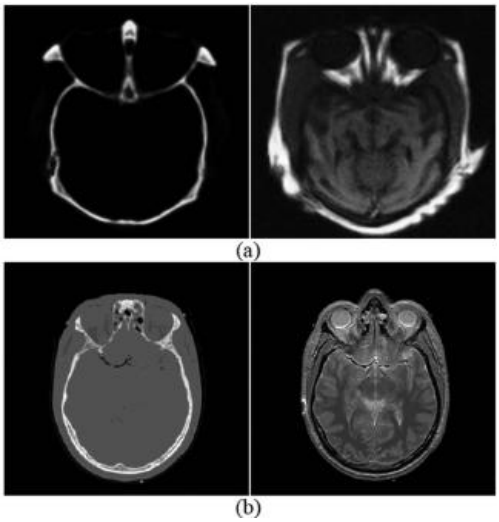

Figure 1. CT and MR images (a) dataset 1 (b) dataset 2

2. LITERATURE SURVEY

An efficient pixel-level image fusion8 algorithm should satisfy the following three requirements:It should preserve the necessary information from input imagery. It should not produce artifacts.It should not depend on location and orientation of the objects present in the source imagery.In this context, for the past few decades, several pixel-level image fusion algorithms have been developed for spatially register images. Pixel-level image fusion can be classified in a generic way based on the methods used, namely, nonlinear operator, optimization, artificial neural network, multiresolution decomposition, and edge preserving-based methods. In nonlinear methods, min, max, and morphological nonlinear operators are used for the purpose of fusion. Successful fusion methods based on morphological operators are discussed in [6]. Even though these methods are simple, fused image may not look good. In optimization-based approaches [7] fusion process is expressed as Bayesian optimization problem. But in general, this problem is difficult to solve. Markov random field [8] and generalized random walk [9] methods solve this problem by computing edge aligned weights. Fused image may be over smoothened because of multiple iterations. Furthermore, artificial neural networks have gained a lot of interest in imagefusion by the inspiration of biological signal fusion. Successful methods in this class are discussed in [10]. In addition to the above fusion schemes, multiresolution schemes have played a great role in image fusion. These schemes are motivated by the fact that human visual system (HVS) is sensitive to the edge information. That is, HVS can perceive even small changes in edge information. Both image pyramid and wavelet decomposition belong to multiresolution methods. These approaches require transform domain analysis. Image pyramid decomposes each given image into set of lowpass filtered images. Each filtered image represents the information of the given image in different scales [11]. Gradient pyramid (Grad) [12],Laplacian pyramid [13], ratio of low-pass pyramid (Ratio) [14], Gaussian pyramid [15],contrast pyramid, filter-subtract-decimate pyramid, and morphological pyramid [16] methods are used for the purpose of fusion.

3. PROPOSED METHOD

3.1. Statistics based guided image filter (SGIF)

The proposed SGIF method is explained as follows:

If $\mathcal{G}$ is a guided image centered at a pixel m in a local square window w, then the filtered output $\mathbb{O}$ at a pixel n is given by

$$\mathbb{O}_n = a_m \mathcal{G}_n + b_m, \forall n \in w_m \quad (1)$$

Where a_m and b_m are the linear coefficients which are constant in window w_m.

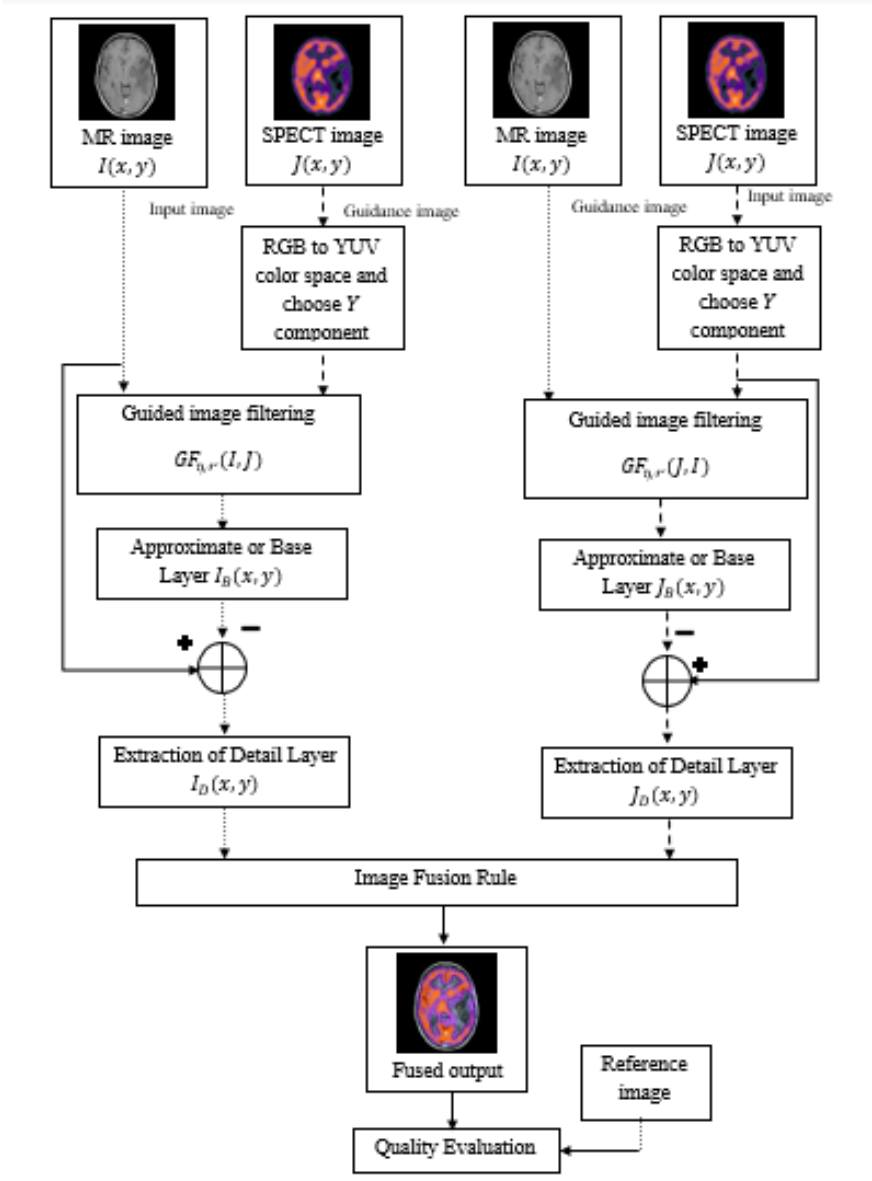

Figure 2. Proposed MR and SPECT image fusion methodology.

To determine linear coefficients, constraints have to be derived from the input image $\mathbb{I}$. In other way, to get noise free output, unwanted components $\mathbb{N}$ (like noise or texture) must be subtracted from $\mathbb{I}$.

$$\mathbb{O}_n = \mathbb{I}_n - \mathbb{N}_n \quad (2)$$

The solution for this problem should minimize the difference between $\mathbb{I}$ and $\mathbb{O}$. It should also maintain the relation in eq. (7). Hence, a_m and b_m are the linear coefficients that can minimize the cost function in window $\mathcal{w}_m$ a

$$E(a_m, b_m) = \sum_{n\in w_m}\{(a_m \mathcal{G}_n + b_m - \mathbb{I}_n)^2 + \mathcal{r} {a_m}^2\} \quad (3)$$

where $\mathcal{r}$ is the regulization parameter. Eq. (3) represents the linear regression model. The solution for this is directly given b

$$a_m = \frac{\frac{1}{|w|}\sum_{n\in w_m} \mathbb{S}_n \mathbb{I}_n - \mu_m \bar{\mathbb{I}}_n}{{\sigma^2}_m + \mathcal{r}} \quad (4)$$

$$b_m = \bar{\mathbb{I}}_n - a_m \mu_m \quad (5)$$

Here $|\mathcal{w}|$ is the number of pixels in a window $\mathcal{w}_m$ centered at pixel $\mathcal{m}$, μ_m is the mean, and ${\sigma^2}_m$ is the variance in the window$\mathcal{w}_m$. $\bar{\mathbb{I}}_n$ is the mean of input $\mathbb{I}_n$in $\mathcal{w}_m$ and is given by

$$\bar{\mathbb{I}}_n = \frac{1}{\mathcal{w}}\sum_{n\in w_m} \mathbb{I}_n \quad (6)$$

Once linear coefficients are obtained, then output $\mathbb{O}_n$ can be solved according to eq. (6). But different overlapping windows $\mathcal{w}_m$ centered at $\mathcal{m}$ contain pixel $\mathcal{n}$ in common. To resolve this problem, take average of all estimates of $\mathbb{O}_n$. Hence, the filtering output can be given as

$$\mathbb{O}_n = \overline{a_m}\mathcal{G}_n + \overline{b_m} \quad (7)$$

Where $\overline{a_m} = \frac{1}{\mathcal{w}}\sum_{n\in w_m} a_m$ and $\overline{b_m} = \frac{1}{\mathcal{w}}\sum_{n\in w_m} b_m$ are the averages of all linear coefficients. In this article, filtering output of guided image $\mathbb{I}$ in the guiding of $\mathcal{G}$ is denoted as$SGIF_{\mathfrak{y},\mathcal{r}}(\mathbb{I}, \mathcal{G})$, where $\mathfrak{y}$ is the filter size/neighborhood size and $\mathcal{r}$ is the degree of smoothing/regulization parameter. The behaviour of the SGIF controlled by these parameters $\mathfrak{y}$ and$\mathcal{r}$. If the guided image has a variance ${\sigma^2}_m$ higher than the threshold$\mathcal{r}({\sigma^2}_m \geq \mathcal{r})$, within a window $\mathcal{w}_m$, then the pixel in the center of the window remain unchanged, whereas if a pixel is in the centre of low variance window whose variance is less than, then pixel value is replaced by the average of the neighbourhood. Some major applications of GF include edge preserving smoothing, image matting, feathering HDR compression, and detail enhancement. Along with edge-preserving filtering, two properties—structure transferring and gradient preserving—make GF qualify for the purpose of image fusion.

3.1.1. Structure transferring filtering

This is one of the important properties of GF. If the guidance image is same as the input image then there is no impact on the structure of input image. However, the guided image is different from the input image then structures of the guidance image influence the input image.

3.1.2. Gradient preserving filtering

Besides edge-preserving filtering like bilateral filter, joint bilateral filters GF can also avoid gradient reversal artifacts during filtering process. Because of these qualities this filter is also used in detail enhancement. In detail enhancement, edge aware smoothing filtered output treated as base layer B for the input I. Detail layerD is computed as Di = Ii - Bi. Manipulated detailed layer is combined with base layer

to get enhanced image. Compared to bilateral filter, guided filter performs better near edges because of gradient preserving.

3.2. Image Fusion Rule

The basic idea is to find weight corresponding to a pixel in an image based on its horizontal and vertical edge strengths. In theory, to find a weight corresponding to a pixel at a location (m, n) in an image take a square window $\mathcal{w}$ of size $p \times p$ around its neighbourhood. Consider $\mathbb{Q}$ as a matrix and find its covariance matrix by considering row as an observation, column as a variable.

$$cov(\mathbb{Q}) = E[(\mathbb{Q} - E[\mathbb{Q}])(\mathbb{Q} - E[\mathbb{Q}])^T] \quad (8)$$

Calculate unbiased horizontal estimate of a covariance matrix at a pixel location (m, n) as

$$\mathfrak{U}_{\mathcal{E}_{\mathrm{H}}}^{m,n}(\mathbb{Q}) = \frac{1}{p-1}\sum_{\hbar=1}^{p}(\mathbb{Q}_{\hbar} - \overline{\mathbb{Q}})(\mathbb{Q}_{\hbar} - \overline{\mathbb{Q}})^T \quad (9)$$

Where $\mathbb{Q}_{\hbar}$ is the $\hbar^{th}$ observation of the p -dimensional variable and $\overline{\mathbb{Q}}$ is the average of the observation. Interestingly diagonal of $\mathfrak{U}_{\mathcal{E}_{\mathrm{H}}}^{m,n}(\mathbb{Q})$ is a variance vector. Compute Eigen values $\lambda_{\mathcal{E}_{\mathrm{H}}}^{\hbar}$ of $\mathfrak{U}_{\mathcal{E}_{\mathrm{H}}}^{m,n}(\mathbb{Q})$. As the size of matrix is $p \times p$, number of Eigen values can be found is p. To get horizontal edge strength $\mathrm{e}_{\mathcal{E}_{\mathrm{H}}}$, add all these Eigen values.

$$\mathrm{e}_{\mathcal{E}_{\mathrm{H}}}(m, n) = \sum_{\hbar=1}^{p}\lambda_{\mathcal{E}_{\mathrm{H}}}^{\hbar} \quad (10)$$

Similarly, to take vertical edge strength into account, take every column as an observation and row as a variable. Calculate the unbiased vertical estimate $\mathfrak{U}_{\mathcal{E}_{\mathcal{V}}}^{m,n}$, and then compute the Eigen values $\lambda_{\mathcal{E}_{\mathcal{V}}}^{\hbar}$. Add these Eigen values to get the vertical edge strength $\mathrm{e}_{\mathcal{E}_{\mathcal{V}}}$ as,

$$\mathrm{e}_{\mathcal{E}_{\mathcal{V}}}(m, n) = \sum_{\hbar=1}^{p}\lambda_{\mathcal{E}_{\mathcal{V}}}^{\hbar} \quad (11)$$

To find the weight $\mathbb{W}(m, n)$of a pixel at location(m, n), take a sum of $\mathrm{e}_{\mathcal{E}_{\mathrm{H}}}(m, n)$ and $\mathrm{e}_{\mathcal{E}_{\mathcal{V}}}(m, n)$

$$\mathbb{W}(m, n) = \mathrm{e}_{\mathcal{E}_{\mathrm{H}}}(m, n) + \mathrm{e}_{\mathcal{E}_{\mathcal{V}}}(m, n) \quad (12)$$

4. RESULTS AND DISCUSSION

All the experiments have been done in MATLAB 2016b version under the high-speed CPU conditions for faster running time. Aim of any fusion algorithm is to integrate required information from both source images in the output image. Fused image cannot be judged exclusively by seeing the output image or by measuring fusion metrics. It should be judged qualitatively using visual display and quantitatively using fusion metrics. In this section, we are presenting both visual quality and quantitative analysis of proposed and existing algorithms such as, Wavelet based methods discrete wavelet transform (DWT), stationary wavelet transform (SWT) and integrated principal component analysis with anisotropic diffusion (IPCA-AD). Analysis of fusion metricsalong with image quality assessment (IQA) metrics such as peak signal-to-noise ratio (PSNR), structural similarity index (SSIM), correlation coefficient (CC), root mean square error (RMSE) and entropy (E) are considered to verify the effectiveness of the proposed algorithm. The objective of any fusion algorithm is to generate a qualitative fused image.For better quality, fused image should have optimal values for all these metrics. The fusion metric with best value is highlighted in bold letter. Visual quality of fused images obtained using state-of-art algorithms such as DWT, SWT and proposed method has demonstrated in figure 3 and figure 4 with data set 1 and data set 2. However, all the

existing fusion methods outputs not good at visual perception, lack of contrast with edge information and texture preservation. Our proposed method which is presented in figure 3 (d) and figure 4(d), which looks more quality in visualization, good contrast with proper edge information and excellent texture preservation as the value of entropy is much higher.

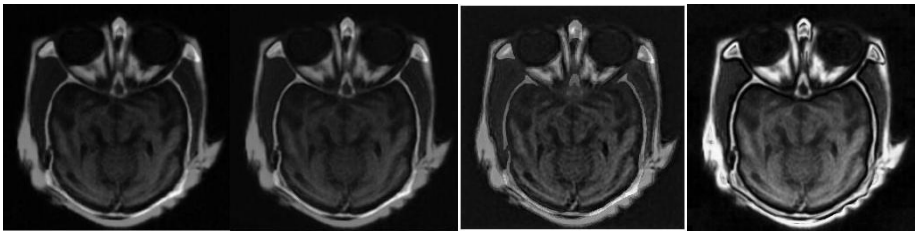

(a)(b)(c)(d)

Fig. 3: Visualization of fused output images with data set 1 (a)DWT (b) SWT(c) IPCA-AD (d) Proposed method.

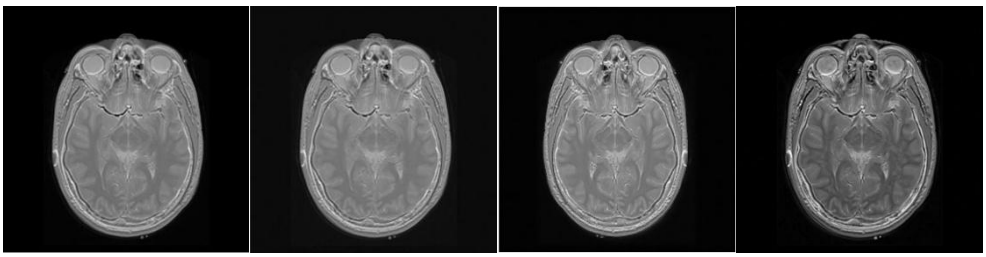

(a)(b)(c)(d)

Fig. 4: Visualization of fused output images with data set 2 (a) DWT (b)SWT (c) IPCA-AD (d)Proposed method.

Table 1: Quantitative analysis of fusion methods for dataset 1.

Methodology	PSNR (in dB)	RMSE	CC	SSIM	Entropy
SWT	62.253	0.1967	0.7928	0.986	6.11
DWT	62.257	0.1966	0.7935	0.986	6.099
IPCA-AD	65.06	0.142	0.913	0.997	6.24
Proposed method	**91.31**	**0.0069**	**0.999**	**1**	**6.98**

Table 2: Quantitative analysis of fusion methods for dataset 2

Methodology	PSNR (in dB)	RMSE	CC	SSIM	Entropy
SWT	68.95	0.0909	0.933	0.988	0.9684
DWT	68.98	0.0906	0.934	0.988	0.9683
IPCA-AD	74.18	0.049	0.973	0.999	5.16
Proposed method	**87.14**	**0.0111**	**0.998**	**0.9999**	**5.22**

Quantitative analysis with IQA sown in table 1 for the test results presented in figure 3, which gives the analysis of dataset 1. Table 1 consists of various fusion metric parameters such as PSNR, RMSE, CC, SSIM and entropy. The best values are highlighted in bold letters. Our proposed method obtained far better values over all the existing fusion methods discussed in the literature. We also tested the qualitative analysis of dataset 2 with the similar fusion metric parameters considered for dataset 1.

Obtained results of MR and SPECT

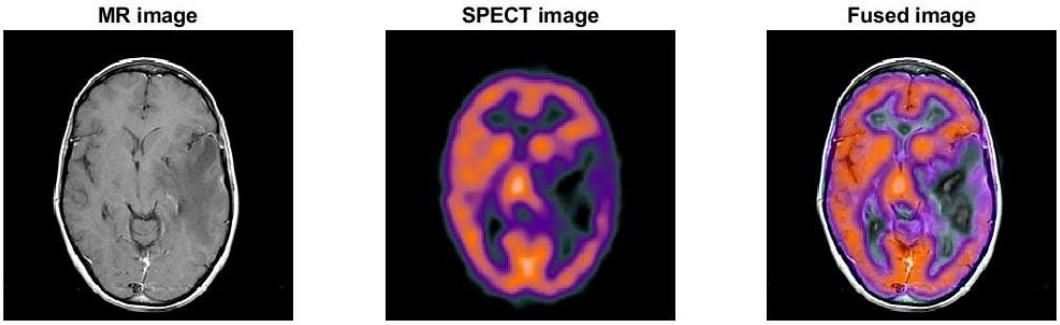

Fig. 5:Obtained fused image of MR and SPECT using proposed method.

Elapsed time is 2.602502 seconds.

The Entropy for Proposed is 4.4625

The Mean for Proposed is 53.8239

The STD for Proposed is 73.8493

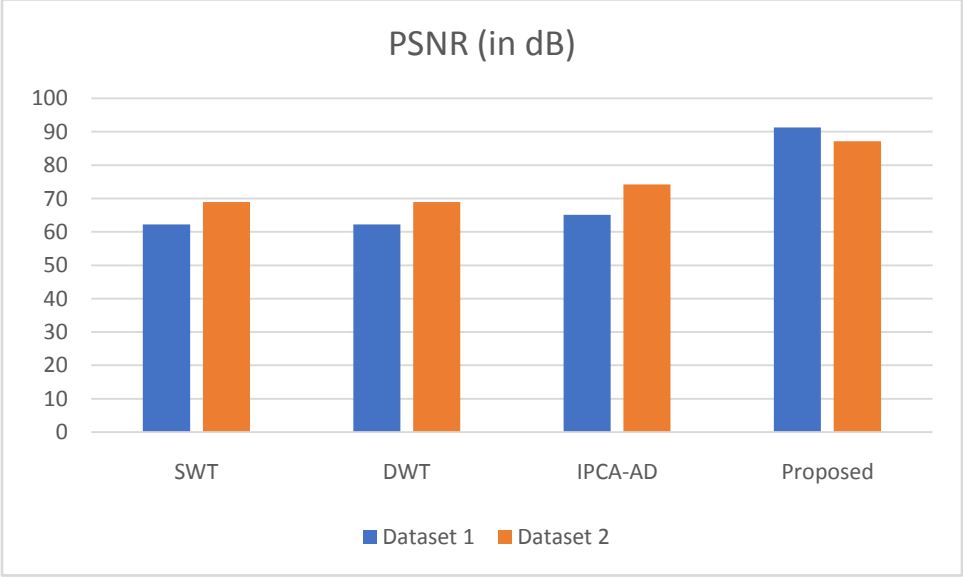

Fig. 6: PSNR comparison of existing and proposed fusion approaches with dataset 1 and dataset 2.

Further, performance evaluation graph of PSNR (in dB)for dataset 1 and dataset 2 is disclosed in Fig. 6 with proposed and existing fusion algorithms. Fig. 7 and Fig. 8 discloses the performance evaluation graph of RMSE, CC, SSIM, and entropy using existing and proposed fusion algorithms for dataset1 and dataset 2.

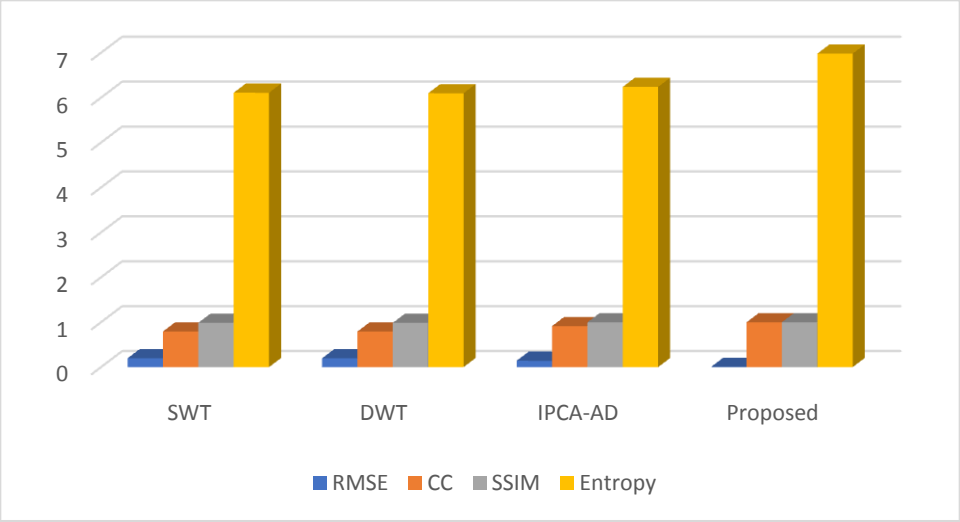

Fig. 7: Performance evaluation graph of RMSE, CC, SSIM, and entropy using existing and proposed fusion algorithms for dataset 1.

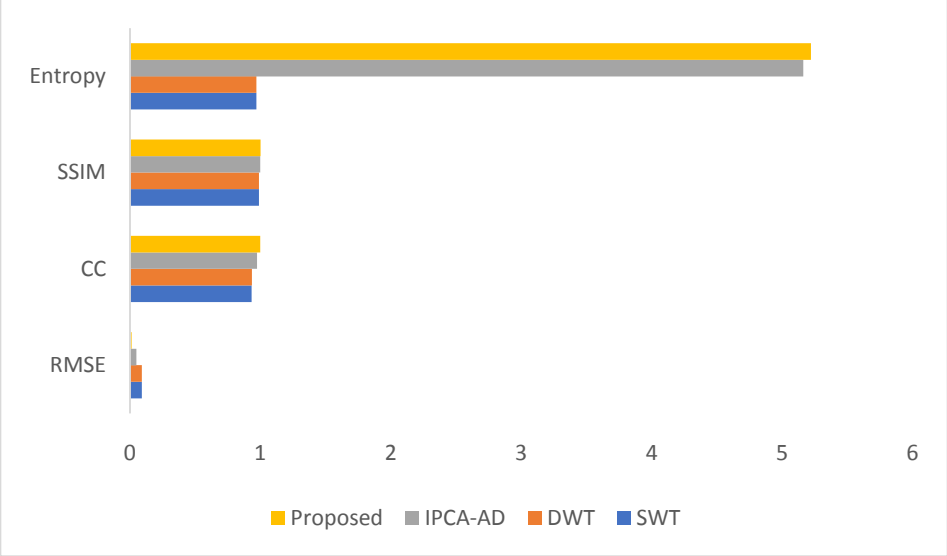

Fig. 8: Performance evaluation graph of RMSE, CC, SSIM, and entropy using existing and proposed fusion algorithms for dataset 2.

5. CONCLUSIONS

A new pixel-level fusion algorithm is proposed to fuse SPECT and MR images. First, each source image is filtered using edge aware smoothing guided filter. Weights are calculated based on statistics of the detail layers. Then fused image is obtained by taking the weighted average of the source images. Fusion performance is assessed in terms of visual quality and evaluation metrics. Results reveal that proposed method is well suited for medical imaging. Our method showed promising results compared to the traditional and recent fusion techniques. Even though experiments are demonstrated for CT and MRI modalities, proposed algorithm can also be applied on other medical imaging modalities as well.In this article, for effective demonstration, results and analysis of two image datasets are presented. However, our fusion method can also yield better performance for a random image fusion dataset of our

choice.Along with medical imaging, proposed method can also give reasonable performance for both single- and multi-sensor image fusion applications.

REFERENCES

[1] Liu S, Zhao J, Shi M. Medical image fusion based on improved sum-modified-Laplacian. Int J ImagSyst Technol. 2015;25:206– 212.no.

[2] Liu S, Zhang T, Li H, Zhao J, Li H. Medical image fusion based on nuclear norm minimization. Int J ImagSyst Technol. 2015;25:310–316.no.

[3] Hamza A, He Y, Krim H, Willsky A. A multiscale approach to pixel-level image fusion. IntegrComput Aid Eng. 2005;12:135– 146. no.

[4] Li H, Manjunath BS, Mitra SK. Multisensor image fusion using the wavelet transform. Graph Models Image Process. 1995;57: 235–245.no.

[5] Petrovic V. Multisensor pixel-level image fusion PhD thesis. In: Department of Imaging Science and Biomedical Engineering Manchester School of Engineering, United Kingdom, 2001.

[6] Sasikala M, Kumaravel N. A comparative analysis of feature based image fusion methods. Information Technol J. 2007;6: 1224–1230. no.

[7] Tao Q, Veldhuis R. Threshold-optimized decision-level fusion and its application to biometrics. Pattern Recognit. 2009;42: 823–836.no.

[8] Aslantas V, Toprak AN. A pixel based multi-focus image fusion method. OptCommun. 2014;332:350–358.

[9] De I, Chanda B, Chattopadhyay B. Enhancing effective depthof-field by image fusion using mathematical morphology. Image Vis Comput. 2006;24:1278–1287.no.

[10] Ramac LC, Uner MK, Varshney PK, Alford MG, Ferris DD Jr. Morphological filters and wavelet-based image fusion for concealed weapons detection. In: Aerospace/Defense Sensing andControls, pp. 110–119. International Society for Optics and Photonics, 1998.

[11] Yang B, Li S. Multi-focus image fusion based on spatial frequency and morphological operators. Chinese Opt Lett. 2007;5: 452–453. no.

[12] Fasbender D, Radoux J, Bogaert P. Bayesian data fusion for adaptable image pansharpening. IEEE Trans Geosci Remote Sens. 2008;46:1847–1857.no.

[13] Mascarenhas NDA, Banon GJF, Candeias ALB. Multispectral image data fusion under a Bayesian approach. Int J Remote Sens. 1996;17:1457–1471.no.

[14] Shen R, Cheng I, Shi J, Basu A. Generalized random walks for fusion of multi-exposure images. IEEE Trans Image Process. 2011;20:3634–3646. no.

[15] Xu M, Chen H, Varshney PK. An image fusion approach based on Markov random fields. IEEE Trans Geosci Remote Sens. 2011;49:5116–5127. no.

[16] Newman EA, Hartline PH. Integration of visual and infrared information in bimodal neurons of the rattlesnake optic tectum. Science (New York, NY). 1981;213:789.

[17] Newman EA, Hartline PH. The infrared “vision” of snakes. Sci Am. 1982.

[18] Schiller PH. The color-opponent and broad-band channels of the primate visual system. In: From Pigments to Perception. US: Springer; 1991: 127–132.

[19] Schiller PH. The ON and OFF channels of the visual system. Trends Neurosci. 1992;15:86–92.no.

[20] Waxman AM, Seibert MC, Gove A, et al. Neural processing of targets in visible, multispectral IR and SAR imagery. Neural Networks. 1995;8:1029–1051.no.